Journal of Manufacturing Engineering, December 2025, Vol. 20, Issue. 4, pp 136-143
DOI: https://doi.org/10.37255/jme.v20i4pp136-143

SIMULATION-DRIVEN DESIGN OPTIMISATION FOR DEFECT-FREE GRAY CAST IRON BRAKE DISCS: AN INDUSTRIAL CASE STUDY

Sajad Sadoughi [a,b*]

[a] Department of Materials Science and Engineering, Sharif University of Technology, Tehran, Iran.
[b] Ex-employee of Parlite Asia Company, Karaj, Iran

Abstract

Gray cast iron brake discs are widely used in automotive applications; however, micro-shrinkage defects that occur during casting can significantly impact their performance. This study addresses this critical issue by combining simulation and experimental validation to optimise the casting design. Using MAGMASOFT® simulation software, the formation of shrinkage porosities in an industrial brake disc was analysed, revealing that thermal concentration at L-junctions between the disc and flange was the primary cause. Three modified designs were proposed, incorporating fillet radii, increased flange inner diameters, and reduced chamfers to redistribute heat and minimise defects. Experimental validation confirmed that Design 3 (9 mm chamfer reduction + 130 mm flange inner diameter) successfully eliminated subsurface porosity without additional feeders or process complexity. This work demonstrates that minor geometric adjustments—rather than costly feeder additions—can effectively mitigate shrinkage defects in sand-cast brake discs, offering a practical solution for foundries.

Keywords: *Gray cast iron, brake disc, shrinkage porosity, simulation, design optimisation, casting defects, MAGMASOFT®*

1. Introduction

Nowadays, brake discs, especially those made of gray cast iron, are a ubiquitous technology in modern vehicles, ensuring the safety of automotive transportation. The mechanical and physiochemical properties of brake discs, such as strength, noise, wear, and braking characteristics, are highly dependent on the metallurgical properties of gray cast iron alloys[1-3](Chun-Ping Yeh, 2009). Therefore, to meet the technical demands, it is highly necessary that both the operation of braking systems and the process of their actual manufacturing should be paid special attention. Mainly because gray cast iron braking discs are manufactured through sand casting, which is followed by machining of individual castings, the proper functioning of brake discs can be controlled by the casting quality of the initial semi-product[2].

Cast irons are a group of ferrous alloys which are highly desirable for the production of casting parts with exceptional resistance towards a thermally-stressed environment for long periods of time[3]. Thanks to their good wear resistance, machinability, castability, and vibration-damping ability, gray cast iron alloys have great potential applications in the manufacturing industry, including but not limited to ships, machine tools, and automobiles [4-8]. The solidification of gray cast iron begins with the participation of primary austenite from the molten state. At the eutectic temperature, nucleation and growth of austenite-graphite cells occur on or adjacent to the primary dendrites, leading to the release of heat and an increase in undercooling [1]. The precipitation of graphite flakes is a key step in the production of gray cast iron alloys. Graphite flakes are soft constituents in the microstructure of cast iron, resulting in a decrease in mechanical strength, reduced casting shrinkage, and improved machinability [1]. According to PN-EN ISO945 (1999) [9], there are eight types of size and five types of arrangement of graphite flakes in gray cast iron alloys. Notably, impurities and alloy additives play a crucial role in the nucleation of graphite flakes during the production of gray cast irons from the melt [10, 11].

The functionality and performance of casting parts are influenced by casting defects, eventually leading to a decrease in efficiency and an increase in costs. Because these defects lead to leaks and breakages, resulting in economic losses for manufacturing plants, defects in casting are detrimental to the functionality of automotive components [2]. One of the significant phenomena incorporated with the casting of cast iron is

**Corresponding Author -E-mail: sajjadsadooghi24@gmail.com*

Journal of Manufacturing Engineering, December 2025, Vol. 20, Issue. 4, pp 136-143
DOI: https://doi.org/10.37255/jme.v20i4pp136-143

the shrinkage of the casting part during solidification [12, 13]. When the cast iron cools to ambient temperature from its liquid state, shrinkage defects form in the matrix of the cast iron material. Notably, the formation of shrinkage and shrinkage porosity is possible through the provision of excess melt from another source, that is, in casting terminology, a feeder[14-16]. The dimensional characteristics and shape of feeders depend mainly on the size of the casting part and the physicochemical properties of the casting alloys[2]. To confine shrinkage and shrinkage porosities in feeders and ensure the soundness of casting parts, it is crucial to design the casting part in a way that facilitates unidirectional solidification [17,18]. The solidification of casting parts involves two main steps; the first one includes the progression of solidification front from the surface of casting parts towards the bulk and the concurrent smooth refilling from the feeders, the second one occurs in a feasible situation that the refilling of metals in the solidification zones are hindered; therefore, the compensation of volume decrease in the solidification of metal is not likely to happen [2], leading to shrinkage defects (Micro shrinkage porosity). Stefanescu et al.[19] claimed that the appearance of microporosity is really close to the dendrite shape in the size of micrometres to hundreds of micrometres.

To mitigate casting defects, manufacturers are utilising simulation and modelling software packages. Computational fluid dynamics (CFD) is a reliable tool for predicting the location and underlying causes of casting defects through the numerical simulation of fluid flow and heat transfer. In recent years, several simulation packages, including ProCAST, OpenFOAM, Fluent, FLOW-3D CAST, and MAGMASOFT, have been developed to predict casting defects. Namchanthra et al.[20] utilised FLOW-3D CAST software and Volume of Fluid (VOF) method to simulate the fluid patterns and solidification of the air-valve casting process. Through the application of simulation, the optimal configuration of the sprue, as well as the quantity and location of feeders/risers, has been proposed. Using NovaFlow & Solid CV 4.6r42 version of Office NovaCasting, Futáš et al.[2] investigated the possibility of the occurrence of shrinkage porosity in a railway brake disk, which was manufactured from ductile cast iron (EN-GJS500-7). The primary objective of the research was not only to decrease the occurrence of shrinkage defects in the casting part but also to reduce casting costs. Futáš et al. attempted to reduce the feeder number from 6 to 1 by optimising the gating system and casting position in the mould. In another study from Futáš et al.[3], It has been claimed that, through the application of the NovaFlow & Solid CV 4.6r42 version of Office NovaCasting, the layout of feeders in the sand mold can be modified in a way that the shrinkage and micro-shrinkage porosities in the ribs of ductile cast iron brake discs (EN-GJS-400-16) are eliminated. Sabík et al.[21] investigated the effect of gating designs on the quality and cost efficiency of a clutch wheel for wind turbines, which was produced from a grade of ductile cast iron (EN-GJS-500-7). Via the NovaFlow & Solid casting simulation package, it has been reported that the defects that occurred during the solidification process have been eliminated. Using a simulation casting package, Kugu et al. [31] investigated the influence of three gating and runner designs on the efficiency and casting defects of an automotive gray cast iron brake disc weighing 4.5 kg. To compare the efficiency of three different gating/runner designs, the Reynolds number was utilised, and the optimised gating design was verified.

According to a literature survey, the most recent studies have focused on the design of gating runners and on the quantity and location of feeders/risers to prevent casting defects, gas entrapment, and shrinkage porosity. However, it is worth mentioning that increasing the number of feeders is a cost-intensive approach to hinder micro-shrinkage porosity. Additionally, due to the complex geometry of the casting part or technical limitations, it would be impossible to consider feeders in the location of micro-shrinkage porosities. Moreover, there is a lack of research about the minor modification of casting part design to reduce micro-shrinkage porosities. In this project, the porosities of gray cast iron automotive brake discs were observed on the surface of the machined part after the machining process, which hindered the practical application of brake discs. In the first step, using the MAGMASOFT package software, it became clear that the primary cause of these porosities is metal contraction during the solidification of the casting parts. In the second step, to address this issue, three designs of the casting part have been proposed, taking into account the functional application of the casting part. In the final step, the optimised casting design was manufactured through sand casting and a subsequent machining process to verify the elimination of micro-shrinkage porosities.

2. Experiment

2.1 Materials and methods

A gray cast iron material (GLJ3 according to PSA S34 5100) was utilised. The sand moulding process was conducted using a DISAMATIC machine with a line code of 240B and a length of 100m. The dimensions of the sand mould were 775 mm x 600 mm x 300 mm. The nucleation of graphite was manipulated through the addition of ferrosilicon inoculation with a weight percentage of 0.1 to molten gray cast iron. The 3D model

Journal of Manufacturing Engineering, December 2025, Vol. 20, Issue. 4, pp 136-143
DOI: https://doi.org/10.37255/jme.v20i4pp136-143

of the casting part with runners and gates, and the drawing of machined brake discs are shown in Fig. 1 (a) and (b), respectively.

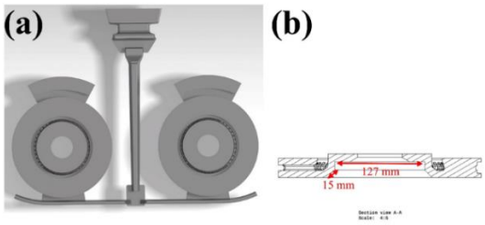

Fig. 1. A representation of (a) casting part with runners and gates and (b) the drawing of a machined brake disc model.

2.2 Material characterisation

To assess the morphology of micro-shrinkage porosities, samples measuring 10 x 10 x 10 mm were cut from the casting part, and a metallographic preparation procedure, including sampling, grinding, and polishing, was conducted. Using SiC grinding papers (from no. 240 to no. 2400), the samples were ground, and then the polishing process was conducted using a 1µm diamond suspension. The micro-shrinkage porosities were investigated using an optical microscope (Olympus DSX-1000 digital microscope). The fully polished samples have been etched using a 2% Nital etch (nitric acid with ethanol). Additionally, the morphology and size of shrinkage porosities were examined using a scanning electron microscope (Hitachi High Technologies) with an accelerating voltage of 16 kV. To tackle charge accumulation, a thin layer of gold was sputtered on the surface of the samples.

2.3. Simulation

The development of a 3D model in SOLIDWORKS was the first step in simulating a casting part using the MAGMASOFT package. The sand-casting mould was designed in-house, utilising the expertise of Asia Pearlite Co. in mould design. Then, the model was imported into MAGMASOFT and was discretised using a cubical mesh. Material properties, including all types of heat transfer (conduction, radiation, and convection), and the solver mode are already coded in the software development. The input parameters of the sand-casting process were specified as shown in Table 1. The initial temperatures of the mould and melt were considered to be 20 °C and 1400 °C. The mould was simulated to identify hot spots, locations of shrinkage porosities, and the liquid fraction. Fig. 2 is a representation of the steps that were followed in succession in all of the simulations in this research.

Table 1 - Input values for the solidification simulation

Row	Value	Reference
Molding material	Silica sand	-
Casting temperature (ºC)	1400	-
Temperature of the mold (ºC)	25	-
Liquidus temperature (ºC)	1200	Jmatpro
Solidus Temperature (ºC)	1125	Jmatpro
Latent heat of fusion (kJ/Kg)	247.41	Jmatpro
Density of the solid (kg/m^3)	7340	Jmatpro
Density of the liquid (kg/m^3)	6730	Jmatpro
Thermal Conductivity of the Solid (W/mK)	29.92	Jmatpro
Thermal Conductivity of the Liquid (W/mK)	33.43	Jmatpro
Specific Heat of the Solid (J/KgK)	500	Jmatpro
Specific Heat of the Liquid (J/KgK)	810	Jmatpro
Surface Tension Coefficient of the Liquid (kg/s^2)	1.534	Jmatpro

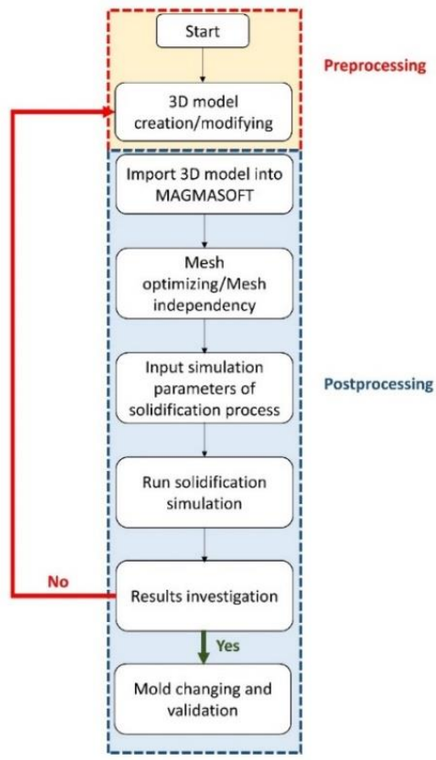

Fig. 2. The block diagram of the automotive brake disc.

Journal of Manufacturing Engineering, December 2025, Vol. 20, Issue. 4, pp 136-143
DOI: https://doi.org/10.37255/jme.v20i4pp136-143

3. Theory of shrinkage porosity calculations

In general, when the temperature of metals falls, the contraction of the metal volume and solidification shrinkage porosities are an undeniable fact. The underlying concept for estimating solidification shrinkage porosities is based on the following procedure [2]. During filling of the mold cavity, molten metal enters the mold; therefore, when the molten metal fills the cavity, the volume of molten metal is identical to that of the mold cavity (V). The volume of molten metal, solidified metal, and solidification shrinkage is as follows[2, 22]:

$$\sum_{i=1}^{n} V_{L(i)} = V, \quad \sum_{i=1}^{n} V_{S(i)} = 0, \quad \sum_{i=1}^{n} V_{shc(i)} = 0 \tag{1}$$

Where n, $V_{L(i)}$, $V_{S(i)}$, and $V_{shc(i)}$ are the total number of nodes, the volume of liquid (m^3), the volume of solid (m^3), and the volume of shrinkage porosities (m^3), respectively. When the temperature of molten metals decreases during the cooling process, the nodal temperatures are controlled at each time step. The reduction in temperature of molten metals just below the liquidus temperature (Θ_L) leading to the initiation of shrinkage porosity formation. The volume of shrinkage porosities is related to the coefficient of solidification shrinkage (S_h). Thanks to the fact that the volume fraction of solid phase (Φ) in time step of t and t+1 is identical; therefore, the volumetric increment of solid phase in the i-th node is as follows[2]:

$$\Delta V_{S(i)} = (\Phi_{S(i)}^{t+1} - \Phi_{S(i)}^{t}) {V_{L(i)}}^{t} \tag{2}$$

The actual nodal volume of solid can be formulated as follows[2]:

$${V_{S(i)}}^{t+1} = \Delta V_{S(i)} + {V_{S(i)}}^{t} \tag{3}$$

Furthermore, the total volumetric increase of solid phase can be defined according to equation (4)[2]:

$$\Delta V_S = \sum_{i=1}^{n} V_{S(i)} \tag{4}$$

Also, the nodal volume of liquid phase can be written as follows[2]:

$${V_{L(i)}}^{t+1} = {V_{L(i)}}^{t} - \Delta V_{S(i)} \tag{5}$$

The corrected content of solid phase in each node can be formulated according to equation (6)[2]:

$$\Phi_{S(i)}^{t+1} = \frac{{V_{S(i)}}^{t+1}}{V_i} \tag{6}$$

The global increment of shrinkage porosities is modeled as follows[2]:

$$\Delta V_{Shc} = \Delta V_S S_h \tag{7}$$

All in all, the above equations at each time step results in the increment in global shrinkage porosities in the casting part.

4. Results and discussion

4.1 Initial mold design for the casting of brake discs

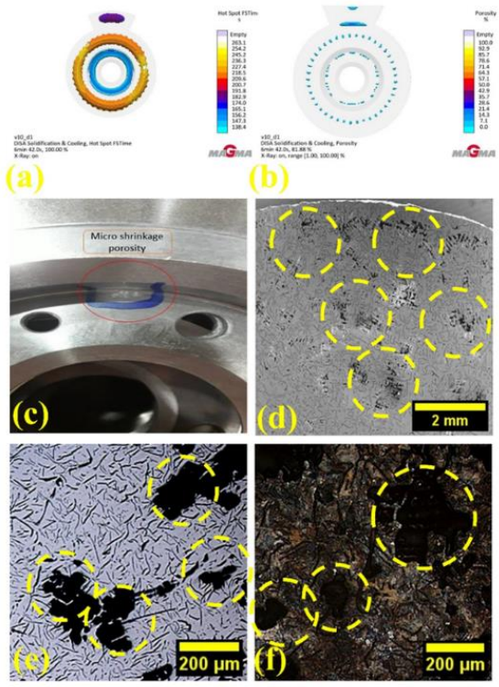

Fig. 3. (a) The micro-shrinkage porosities in the macro scale. (b) A SEM micrograph from the surface of the part after machining. Metallographic image from the surface of part (c) before and (d) after chemical etching. The Magma simulation results of (e) hot spots and (f) shrinkage porosities.

The simulation results of MAGMASOFT software, that is, the hot spots and the location of shrinkage porosities, have been shown in Fig.1-(a) and (b). As can be seen in Fig.1 (a), the areas of the rotor (the disc), the areas adjacent to the flange of the brake disc, and the feeder. Notably, the areas of the flange are critical surfaces, which will be machined immediately after casting to achieve the desired flatness and roughness. Therefore, it is feasible that, after the machining process, these shrinkage porosities, which are undesired defects, become visible on the surface of the brake disc flanges. Additionally, the simulation results for shrinkage porosities, shown in Fig. 1(b), confirmed the possibility of shrinkage porosities occurring in the sand-casting of brake discs. To validate the simulation results, the casting process was conducted on the casting line using the same

Journal of Manufacturing Engineering, December 2025, Vol. 20, Issue. 4, pp 136-143
DOI: https://doi.org/10.37255/jme.v20i4pp136-143

parameters as those simulated. After the casting process, the brake discs have been machined using a CNC machining device. As shown in Fig. 1(c), the accumulation of casting defects, which can include shrinkage porosities, is visible. To investigate the casting defects on the casting, the extracted samples were thoroughly examined using scanning electron microscopy and optical microscopy. The SEM micrograph of the sample in Fig. 3(d) shows a large number of micro-porosities, surrounded by yellow-dashed circles, which accumulate in a wide area of the part, measuring approximately 1 mm in size. The optical microscopy images before and after etching are shown in Fig. 3-(e) and (f), respectively. As shown in Fig. 3(e), the sample's microstructure consists of graphite flakes with a uniform distribution and random orientation, which is consistent with Class I in the ISO 945 standard. Therefore, thanks to the addition of ferrosilicon inoculation, it is highly clear that the nucleation and growth of graphitic flakes happened efficiently. As shown in Fig. 3(f), the sample matrix exhibits a full-pearlitic structure that surrounds graphitic flakes, which is consistent with the standard of PSA S34 5100. The size of micro-shrinkage porosities is around 50 to 100 µm. The morphology of micro-shrinkage porosities is identical to that reported in previous studies. According to previous studies, the junction of the sections increases the mass of molten metal, eventually leading to high thermal gradients around the L junctions. Therefore, to hinder hot spots in L junctions, it is highly desirable to create adequate fillets in the corners [23-27].

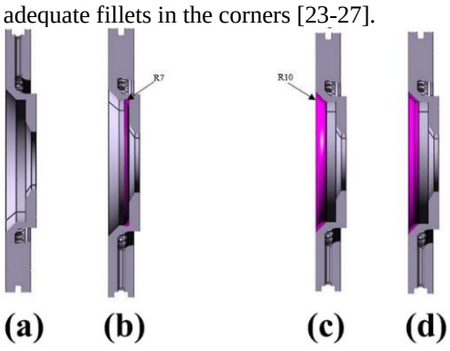

Fig. 4. The cross-sectional graphs of (a) the original design, (b) Design 1: a fillet with a radius of 7 mm has been applied to the L junction and the inner diameter of flange has been increased from 127 mm into 130 mm, (c) Design 2: a fillet with a radius of 10 mm has been applied to the bulging corner of rotor and the inner diameter of flange has been increased from 127 mm into 130 mm, and (d) Design 3: The inner chamfer between rotor and flange has been reduced from 15 mm into 9 mm and the inner diameter of flange has been increased from 127 mm into 130 mm.

As shown in Fig. 4, the junction between the rotor (the disc) and the flange is a type of L junction, which induces hot spots in the junction and subsurface micro-shrinkage porosities. Therefore, to reduce the hot spot around the flange, three designs have been proposed; design (1): a fillet with a radius of 7 mm has been applied to the L junction and the inner diameter of flange has been increased from 127 mm into 130 mm (Fig. 4-(b)), design (2): a fillet with a radius of 10 mm has been applied to the bulging corner of rotor and the inner diameter of flange has been increased from 127 mm into 130 mm (Fig. 4-(c)), and design (3): The inner chamfer between rotor and flange has been reduced from 15 mm into 9 mm and the inner diameter of flange has been increased from 127 mm into 130 mm (Fig. 4-(d)). The purpose of the proposed designs was to control the hot spot around the L junctions and transfer it to low-risk functional areas without the need for a machining cycle end.

4.2 The simulation of proposed brake disc designs

As described, the meeting of two or more walls (elements) in the casting parts will give rise to the thermal concentration in casting parts; therefore, even though the areas adjacent to the junction solidify (due to lower thermal concentration), the molten metals in the conjunctions remain in a liquid state and are prone to shrinkage porosities. The size and extent of defect region (shrinkage porosities) in junctions highly depend on the number of elements (walls) and their thickness, which affect the heat transfer of casting. According to previous studies, the application of feeders/risers on the junction, or a chill below the junction, to remove these defects, is an undeniable action. However, these changes increase the cost of production and the complexity of the process; additionally, due to functional constraints, it is impossible to utilise feeders and chills [23, 24, 26, 27]. Therefore, in this section, the hot spots and shrinkage porosities, as shown in Fig. 5, in the three proposed designs will be evaluated. Fig. 5 (a) and (b) show the locations of hot spots and shrinkage porosities in Design 2. As can be seen in Fig. 5-(a) and (b) and the cross-section of brake discs in Fig. 4-(b), the addition of a fillet with a radius of 7 mm to the L junction and the change inner diameter of flange has not been effective sufficient to decrease the heat concentration around the flange, where micro-shrinkage porosities occurred in the original design. The underlying purpose of Design 2 and Design 3 was to increase the thickness of the bulging corner of the rotor, thereby reducing heat concentration around the flange areas. As can be seen in Fig. 5-(c), (d), (e), and (f), the concurrent effect of the increment in the inner diameter of flange and increase in thickness of rotor bulging area induce larger thicknesses around the bulging area and lower thicknesses

Journal of Manufacturing Engineering, December 2025, Vol. 20, Issue. 4, pp 136-143
DOI: https://doi.org/10.37255/jme.v20i4pp136-143

in flanges; therefore, both the heat concentration around the flange and the possibilities of shrinkage porosities have been reduced efficiently. To validate the prediction of MAGMASOFT, A batch of casting.

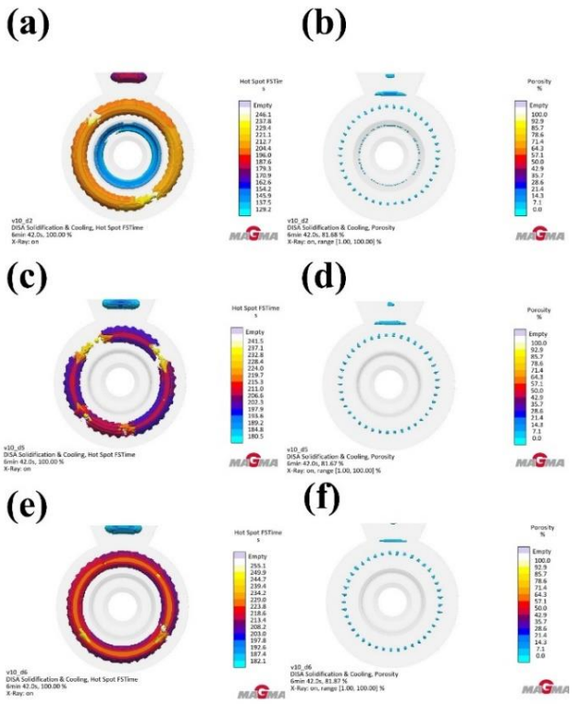

Fig. 5. The hot spot areas of (a) Design 2, (c) Design 3, and (e) Design 4. The micro-shrinkage porosity locations in (b) Design 2, (d) Design 3, and (f) Design 4.

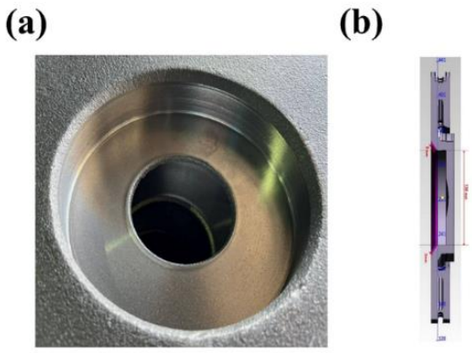

Fig. 6. (a) The image of a machined brake disc with the proposed design of 3. (b) The design parameters of the brake disc with the design of 3.

Design 3 has been manufactured through the casting line, taking into account simulation parameters such as pouring temperature and mould temperature. Fig. 6-(a) and (b) present the casting Design 3 (after machining) and design features of casting Design 3. As shown in Fig. 6(a), the shrinkage porosities have been removed from the areas around the brake disc flange. Mainly due to lower machining cycle and lower manufacturing process, Design 3 has been selected for mass production.

5. Conclusion

This study successfully addressed the critical issue of micro-shrinkage porosity in gray cast iron brake discs through a simulation-driven design optimisation approach. By leveraging MAGMASOFT® simulations, we identified the root cause of defects in the original casting design and systematically developed three improved geometries to eliminate porosity formation. The optimised design, featuring strategic fillet radii and dimensional adjustments, demonstrated complete elimination of shrinkage defects while preserving the required mechanical properties and microstructure.

Key achievements include:

- Defect-free castings achieved through minor geometric modifications, avoiding costly process changes.
- Experimental validation confirming the simulation results, with microstructure analysis showing uniform graphite distribution and no porosity.
- A practical, cost-effective solution for foundries to enhance casting quality without additional feeders or complex adjustments.

This work provides a reliable framework for tackling similar casting defects in industrial applications, highlighting the power of simulation-guided design in manufacturing optimisation. Future studies could explore additional alloy systems or larger-scale industrial validation to further refine this approach.

Acknowledgements

The author would like to express their sincere gratitude to Asia Pearlite Co. for their invaluable industrial support, which included providing production facilities and expertise in the sand-casting process, crucial for the experimental validation of this research. Special thanks are also extended to MAGMA GmbH for providing access to the MAGMASOFT simulation software and their technical support, which enabled the detailed analysis and design optimisation performed in this study.

Author contributions: CRediT

Sajad Sadoughi: Conceptualisation, Formal analysis, Investigation, Methodology, Software, Validation, Visualisation, Writing – original draft, Data curation.

Data Availability

The authors confirm that the data supporting the findings of this study are available within the article [and/or] its supplementary materials.

Reference

1. *C.-P. Yeh, W.-S. Hwang, and C.-H. Lin, "Numerical simulation on hardness distribution for an FC250 gray cast iron brake disc casting and its experimental verification," Materials Transactions, vol. 50, no. 11, pp. 2584–2592, 2009.*
2. *P. Futáš, A. Pribulová, G. Fedorko, V. Molnár, A. Junáková, and V. Laskovský, "Failure analysis of a railway brake disc with the use of casting process simulation," Engineering Failure Analysis, vol. 95, pp. 226–238, 2019.*
3. *P. Futáš, A. Pribulová, V. Šabík, J. Petrík, P. Blaško, and M. Brzeziński, "Elimination of shrinkage in ductile iron castings using computer simulation of casting and solidification," Processes, vol. 12, no. 3, Art. no. 506, 2024.*
4. *X. Cao, Q. Zhang, J. Yu, and X. Yu, "Effect of compositional changes and heat treatment on microstructure and mechanical properties of gray cast iron," Journal of Materials Research and Technology, vol. 35, pp. 5336–5352, 2025.*
5. *N. Kepczak and W. Pawlowski, "Cast iron machine tool body analysis: The theoretical and experimental approach," Iranian Journal of Science and Technology, Transactions of Mechanical Engineering, vol. 44, no. 2, pp. 523–532, 2020.*
6. *M. A. Essam, A. Y. Shash, H. Megahed, and E. El-Kashif, "Effect of section thickness on microstructure and mechanical properties of compacted graphite iron for diesel engine applications," Heliyon, vol. 7, no. 1, Art. no. e05962, 2021.*
7. *Y.-L. Li, Q. Wang, R.-R. Chen, X.-X. Wang, Y. Xia, G.-P. Zhou, Y.-D. Qu, and G.-L. Li, "Influence of V content on microstructure and mechanical properties of gray cast iron for super-large cylinder liner," International Journal of Metalcasting, vol. 17, no. 3, pp. 1806–1814, 2023.*
8. *S. Du, C. Chen, R. Chen, Q. Wang, X. Cui, and Q. Song, "Influence of casting materials on the microstructure and mechanical properties of gray cast iron for cylinder liners," International Journal of Metalcasting, vol. 19, no. 3, pp. 1650–1662, 2025.*
9. *ASTM A247, Standard Test Method for Evaluating Microstructure of Graphite in Iron Castings. West Conshohocken, PA, USA: ASTM International, 1998.*
10. *M. Drajewicz, P. Cichosz, and S. Rudy, "Coupled numerical simulations of the SIMCENTER 3D for casting equipment made of gray cast iron," International Journal of Mechanical Engineering and Robotics Research, vol. 9, no. 10, pp. 1360–1364, 2020.*
11. *L. Dobrzański, Fundamentals of Materials Science and Physical Metallurgy. Warszawa, Poland: WNT, 2002.*
12. *C. Labrecque and M. Gagné, "Ductile iron: Fifty years of continuous development," Canadian Metallurgical Quarterly, vol. 37, no. 5, pp. 343–378, 1998.*
13. *M. Holtzer, R. Dańko, and M. Górny, "Influence of furfuryl molding sand on flake graphite formation in surface layer of ductile iron castings," International Journal of Cast Metals Research, vol. 29, nos. 1–2, pp. 17–25, 2016.*
14. *H. Hou, G. W. Zhang, H. K. Mao, and J. Cheng, "A new prediction way to shrinkage cavity formation for ductile iron castings," in Materials Science Forum. Switzerland: Trans Tech Publications, 2008, pp. 127–134.*
15. *J. Li and B. Li, "Study of solidification shrinkage of ductile iron in dry sand molds," Materials Science and Technology, vol. 15, no. 3, p. 245, 1999.*
16. *P. Larrañaga, J. Gutiérrez, A. Loizaga, J. Sertucha, and R. Suárez, "A computer-aided system for melt quality and shrinkage propensity evaluation based on the solidification process of ductile iron," AFS Transactions, vol. 116, pp. 547–561, 2008.*
17. *A. Skoogh and B. Johansson, "A methodology for input data management in discrete event simulation projects," in Proceedings of the 2008 Winter Simulation Conference. Piscataway, NJ, USA: IEEE, 2008, pp. 1727–1735.*
18. *S. H. Davis, Theory of Solidification. Cambridge, U.K.: Cambridge University Press, 2001.*
19. *D. M. Stefanescu, "Computer simulation of shrinkage-related defects in metal castings—A review," International Journal of Cast Metals Research, vol. 18, no. 3, pp. 129–143, 2005.*
20. *S. Namchanthra, P. Phirommark, T. Phengpom, J. Priyadumkol, W. Wijitdamkerng, W. Chookaew, C. Suvanjumrat, and M. Promtong, "Numerical analysis of molten iron flow and heat transfer in plumbing casting defect detection using split tracking approach," Case Studies in Thermal Engineering, Art. no. 106287, 2025.*
21. *V. Šabík, P. Futáš, and A. Pribulová, "Failure analysis of a clutch wheel for wind turbines with the use of casting process simulation," Engineering Failure Analysis, vol. 135, Art. no. 106159, 2022.*
22. *L. Sowa, "Mathematical model of solidification of the axisymmetric casting while taking into account its shrinkage," Journal of Applied Mathematics and Computational Mechanics, vol. 13, no. 4, pp. 93–102, 2014.*
23. *D. Joshi and B. Ravi, "Classification and simulation-based design of 3D junctions in castings," AFS Transactions, vol. 117, pp. 7–22, 2009.*
24. *K. Singh, P. K. Reddy, D. Joshi, K. Subburaj, and B. Ravi, "3D junctions in castings: Simulation-based DFM analysis and guidelines," in Proceedings of the INAE International*

Conference on Advances in Manufacturing Technology, 2008.

25. *J. B. Caine, Design of Ferrous Castings. New York, NY, USA, 1963.*

26. *W. Jackson, "The design and properties of steel castings: Part 1—Engineering design and design for castability," Materials & Design, vol. 2, no. 4, pp. 187–195, 1981.*

27. *W. Jackson, "The design and properties of steel castings: Part 2—Processing and steel selection," Materials & Design, vol. 2, no. 5, pp. 230–235, 1981.*

